https://doi.org/10.5194/egusphere-2025-6232
Preprint. Discussion started: 12 February 2026

Brief communication: Anthropogenic aerosol forcing of European windstorms in CMIP6 climate models

Stephen Cusack

Stormwise Ltd, Luton, LU4 9DU, United Kingdom

Correspondence to: Stephen Cusack (stephen.cusack@stormwise.co.uk)

Abstract.

A recently developed set of historical storm reconstructions, which were extensively validated by insurance loss data, revealed how European windstorm damages were three times higher in the 1980s and '90s compared to a few decades before and since. A better understanding of these slower fluctuations could improve how this costly risk is managed. Here, we explore the impacts of anthropogenic aerosols (AA) on European property damage using results from DAMIP (Detection and Attribution Model Intercomparison Project) climate model experiments. Multimodel mean DAMIP results indicate AA boosted European wind losses by 45% in the late 20th century relative to preindustrial times, with the signal varying from zero to 100% between the six models. A review of results from previous climate studies suggested the signal is more likely to be at the higher end of this range, though significant uncertainties remain. The results indicate AA forcing could have been a major driver of recent multidecadal changes in European windstorm losses. Further research into observational and modelling uncertainties would benefit those exposed to this risk.

1 Introduction

European windstorm activity has varied at multidecadal scales over the past few centuries (e.g. Dawson et al., 1997; WASA Group, 1998; Brázdil et al., 2004; Mellado-Cano et al., 2019; Hu et al., 2022; Brönnimann et al., 2025). The most recent and best-documented variations in storminess were particularly large, with average property damages (indexed to 2022) rising from €2.8 Bn in 1960-1979 to €6.7 Bn in 1980-1999, before falling to €2.5 Bn in 2000-2019, based on the storm loss reconstructions in Cusack (2023).

Research into these long-timescale changes in European wind climate has identified four main drivers, namely major tropical volcanic eruptions, internal climate variability, solar variations, and anthropogenic aerosol forcing. The evidence pointing to their impacts on multidecadal storminess is now summarized.

The first driver to be considered is major volcanic eruptions injecting huge amounts of sulphur into the tropical stratosphere. Empirical studies of a variety of climate reconstructions suggest this type of volcanic eruption strengthens the European winter wind climate at multiannual (e.g. Groisman, 1992; Robock and Mao, 1995; Shindell et al., 2004; Fischer et al., 2007; Ortega et al., 2015; Birkel et al., 2018; Brönnimann et al., 2025; Orme et al., 2025) and decadal timescales (Dawson et al., 1997;

https://doi.org/10.5194/egusphere-2025-6232
Preprint. Discussion started: 12 February 2026

Zanchettin et al., 2013). Further, the quasi-periodicity of major tropical volcanic eruptions over the past 600 years (Ammann and Naveau, 2003) has coincided with the phase and timescale of multidecadal variations of climate in the North Atlantic sector (e.g. Otterå et al., 2010; Mann et al., 2021; Dai et al., 2022). More detailed analysis has identified the mechanisms connecting eruptions to stormier conditions (e.g. Robock, 2000; Stenchikov et al., 2009; Mignot et al., 2011).

Climate models consistently produce slower climate variations in the North Atlantic sector in the absence of all external forcings, which is referred to as internal variability (e.g. Zhang et al., 2019; Fang et al., 2021). This multidecadal driver can be broken down into two different components. The first concerns the Atlantic Meridional Overturning Circulation (AMOC) system of currents flowing through the full depth of the Atlantic Ocean. Variations in AMOC strength cause changes in northward heat transport (e.g. Yan et al., 2018; Robson et al., 2023), which alter meridional heat gradients in the northern Atlantic, which in turn modulate storminess in the overlying atmosphere (e.g. Brayshaw et al., 2009; Gastineau and Frankignoul, 2012; Peings and Magnusdottir, 2014; Omrani et al., 2014; Woollings et al., 2015). The mechanisms that cause decadal-scale variations in AMOC are not fully understood, though anomalous atmosphere forcing over the northern Atlantic is considered critical (e.g. Böning et al., 2006; Buckley & Marshall, 2016). The second component is atmosphere-based, and consists of shorter-timescale extremes of sufficient magnitude to alter multidecadal averages of storminess. This could be due to extremes in phenomena which drive shorter-timescale variations, such as the Quasi-Biennial Oscillation (QBO; Baldwin et al., 2001), El Niño-Southern Oscillation (ENSO; Brönnimann, 2007) and the 11-year solar cycle (Gray et al., 2016), and their interactions (Labitzke and Kunze, 2009). In addition, the rare chance that weather conditions conducive to extreme events also hit large exposure centres can affect multidecadal-mean losses.

There is a significant amount of evidence that the main 11-year solar cycle drives changes in European winter winds (e.g. Ineson et al., 2011; Scaife et al., 2013; Thiéblemont et al., 2015; Gray et al., 2016; Kuroda et al., 2022). The amplitudes of solar cycles vary at century timescales, and influence European winter climate (e.g. Otterå et al., 2010; Wang et al., 2017). This driver appears to be a minor contributor to storm changes over the past several decades, because the modulation of recent solar cycles corresponds to weak forcing (e.g. Figure 2.10 of Gulev et al., 2021), and was out-of-phase with the multidecadal rise in storminess during the second half of the 20th century.

Anthropogenic aerosols (AA) exerted a large influence on temperatures in the North Atlantic (e.g. Booth et al., 2012) and Arctic (e.g. Aizawa et al., 2022) regions in the 20th century, and recent research indicates their influence extends to European wind climate. For example, Qin et al. (2020) found steeper meridional surface pressure gradients over Europe in the late 20th century in the multimodel means from both the fifth and sixth phases of the Coupled Model Intercomparison Project (CMIP5 and CMIP6, e.g. Eyring et al., 2016). Hassan et al. (2021) found declines in AA from 1990 to 2020 caused about one-third of the observed slackening of pressure gradients between the subpolar Atlantic and Mediterranean areas, in CMIP6 simulations. Needham and Randall (2023) and Needham et al. (2024) analysed a large ensemble of simulations from multiple forcing experiments, and found changes in AA emissions over North America and Europe caused a strengthening storm track in northern mid-latitudes over the second half of the 20th century, and subsequent weakening this century. Observed multidecadal changes in European storm losses align with the AA-forced signals.

https://doi.org/10.5194/egusphere-2025-6232
Preprint. Discussion started: 12 February 2026

The size of AA forcing of storminess is of particular interest to those exposed to wind risk, because future aerosol emissions from northern mid-latitudes are regarded as more predictable than those from natural forcings. Empirical analysis has a fundamental difficulty distinguishing AA forcing from multiple other drivers during the relatively short multidecadal period in which AA forcing was strong. Therefore, in this study, we use climate models to quantify the AA forcing of European storminess. Near-surface winds from the DAMIP (Detection and Attribution Model Intercomparison Project) set of climate model experiments (Gillett et al., 2016) were processed into storm events, then an established model converted these event winds into property losses of concern to the insurance industry. The contribution of AA forcing was found by comparing DAMIP-AA results to control simulations with external forcings set to preindustrial values. Section 2 contains a description of the DAMIP climate model experiments, and the conversion of their near-surface winds to European storm losses. Results from the DAMIP-AA model experiments are presented in Section 3, then explored further in Section 4, with the aid of additional information from previously published research. Conclusions are given in Section 5.

2 Data and methods

2.1 DAMIP climate model data

CMIP6 includes a series of 23 sub-projects targeting specific questions about the climate. In particular, the DAMIP sub-project was designed to measure the relative roles of various climate forcings during the industrial period. Its Tier 1 experiments consist of climate model simulations covering the 1850-2014 period, with one type of forcing set to historical values and all others fixed at preindustrial values, and initial conditions from corresponding preindustrial control runs (from the main climate model experiments of CMIP6). We focus here on results from the DAMIP Tier 1 test of AA forcings. This study used climate models from six different modeling centres with the necessary diagnostics for at least five different ensemble members for the Tier 1 test, at the time of download in July and August 2024. Table 1 summarizes the models and simulations.

Gillett et al. (2016) suggested that starting conditions for different ensemble members be taken from well-separated states of the long Control integration. The historical AA forcings for the forced simulations are based on inventories in the Community Emissions Data System described in Hoesly et al. (2018), with associated radiative forcings described in several studies (e.g. Lund et al., 2018, 2019; Gulev et al., 2021; Bauer et al., 2022). In brief, sulphates have produced the largest radiative forcings in the industrial period, growing from a relatively small amount at the start of the 20th century to peaks in the 1980s and 1990s. The main source regions for 20th century sulphates were Europe, Russia, and to a lesser extent North America (e.g. Lund et al., 2019). There have been large cuts in sulphate emissions from these territories since the late 20th century leading to smaller burdens this century. This is notable, since studies such as Diao et al. (2021) and Needham and Randall (2023) found the strength of the storm track in the northern hemisphere was more sensitive to emissions from mid-latitude regions.

https://doi.org/10.5194/egusphere-2025-6232
Preprint. Discussion started: 12 February 2026

Table 1. Summary details of DAMIP-AA climate model simulations analysed in this study.

Model	No. of ensemble members	Control length (yr)	Atmosphere resolution Horizontal cells; vertical levels	Ocean resolution (km)
CMCC-CM2-SR5	8	500	288 x 192; 30 levs to ~ 2 hPa	100
CanESM5	9	600	128 x 64; 49 levs to 1 hPa	100
HadGEM3-GC31-LL	15	500	192 x 144; 85 levs to ~ 0.01 hPa	100
MIROC6	10	500	256 x 128; 81 levs to 0.004 hPa	100
MPI-ESM1-2-LR	15	600	192 x 96; 47 levs to 0.01 hPa	250
MRI-ESM2-0	5	250	320 x 160; 80 levs to 0.01 hPa	100

2.2 Converting Model Winds to Losses

Windstorm losses in climate simulations were estimated using a method published by Klawa and Ulbrich (2003). Results from the method were validated by a long timeseries of insurance losses which led to its widespread use (e.g. Leckebusch et al., 2007; Pinto et al., 2007; Karremann et al., 2014; Priestley et al., 2024). A brief overview of their method is now given.

Daily maximum near-surface (10 m) winds in the October to April windstorm season were extracted from model simulations for every grid cell in a study domain consisting of 16 countries in northern and central Europe which experience the vast majority of all insured wind losses, shown in Figure 1. The 98th percentile of the daily maximum wind was computed for each simulation, then a proxy of wind damage (D_d) in day d for the whole domain was defined as:

$$D_d = \sum_{i=1}^{N} \left[max\left(\frac{v_{i,d}}{v_{i,98}} - 1, 0 \right) \right]^3$$

where there are N grid cells in the domain, $v_{i,d}$ is the daily maximum wind for the i'th grid cell on day d, and $v_{i,98}$ is the climatological 98th percentile of wind for the i'th grid cell. Storm events (s) are then defined as a series of up to three days centred on the days with peak values of D_d, and the event maximum wind ($v_{i,s}$) is set to the maximum of the daily values comprising the storm, for each grid cell.

Finally, domain-wide event losses were estimated from the storm-maximum winds:

$$L_s = c. \sum_{i=1}^{N} P_i \left[max\left(\frac{v_{i,s}}{v_{i,98}} - 1, 0 \right) \right]^3$$

where L_s is the loss for storm s, and P_i is the population count for the i'th cell from Gridded Population of the World, version 4, at 2.5 minutes of arc resolution (CIESIN, 2018). The constant of proportionality (c) in the above loss equation was used by

https://doi.org/10.5194/egusphere-2025-6232
Preprint. Discussion started: 12 February 2026

KU03 to re-scale their index values to actual loss data. This study analysed the *relative change* in losses, and setting this coefficient to unity does not alter results.

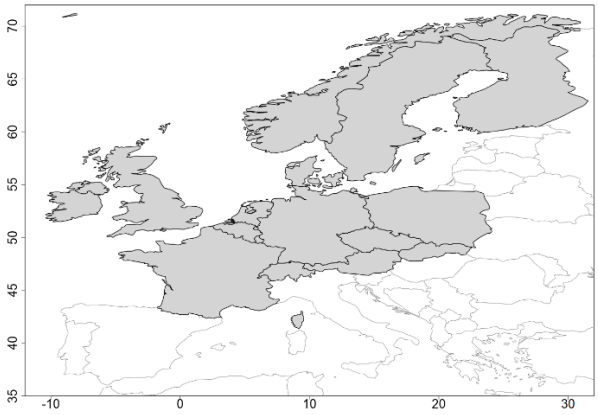

Figure 1: A map of Europe with grey shading highlighting the region for which losses were computed.

Losses from a model simulation with AA forcing were converted to anomalies using the appropriate control simulation, then grouped into ensemble means for each model, and the multimodel mean too, using linear averaging. Subsequently, the storm anomalies were filtered using a low-frequency second-order Butterworth filter with a 20-year cutoff, to highlight the multidecadal timescale of variation in results.

Uncertainties due to sampling errors have been estimated using the standard error of the mean, as follows. The standard deviation of the annual storm anomaly for model m (σ_m) is computed using the full timeseries of annual means from each model's Control run, then the standard error ($\varepsilon_{m,N}$) of its N-year model mean is given as σ_m divided by the square root of N. The standard error of the N-year multimodel mean anomaly is computed similarly, with adjustments for the varying number of members per model (Table 1).

3 Results

Figure 2a shows the timeseries of multimodel mean change in Europe-wide storm losses due to AA forcing, based on all 62 DAMIP-AA simulations. The main feature is a DAMIP-AA model peak at the end of the 20th century with 45% greater windstorm losses than its preindustrial control run; the model signal is at least four standard errors above zero throughout the last two decades of the 20th century and indicates significant increases in European windstorm losses due to AA forcing.

AA-forced anomalies were computed for individual model ensemble-means, and shown in Figure 2b. A t-test was performed on the null hypothesis that each model's mean anomaly was zero, using the longer 1970-2009 period for more robust results. In more detail, the t-test takes ensemble-mean loss anomalies for each year in the 1970-2009 period as input, then assesses

https://doi.org/10.5194/egusphere-2025-6232
Preprint. Discussion started: 12 February 2026

whether the mean value over the whole period is consistent with no response, given the variability of annual anomalies. The p-values of the null hypothesis for each model, given in parentheses in the legend of Figure 2b, indicate four models with a signal above zero at the 99.9% confidence level, including two models projecting a near-certain increase in storm loss due to AA. However, two models simulate no significant AA forcing on European storm losses. At this point in the analysis, there is no evidence to prefer one model over another, and the fact that only four of six have a significant signal suggests AA forcing of storminess is likely, but less certain than that portrayed by the multimodel mean change in Figure 2a. It can be seen from Figure 2b that the size of the multimodel mean signal is mainly due to strong AA forcing of storminess in two of the six models (CanESM5 and HadGEM3-GC31-LL). This wide range of storm responses to AA forcing indicates large uncertainty in the amplitude of the AA signal, and a key feature of model results. Additional information on the AA forcing and climate responses in the six models will be presented in Section 4, to reduce this uncertainty in results.

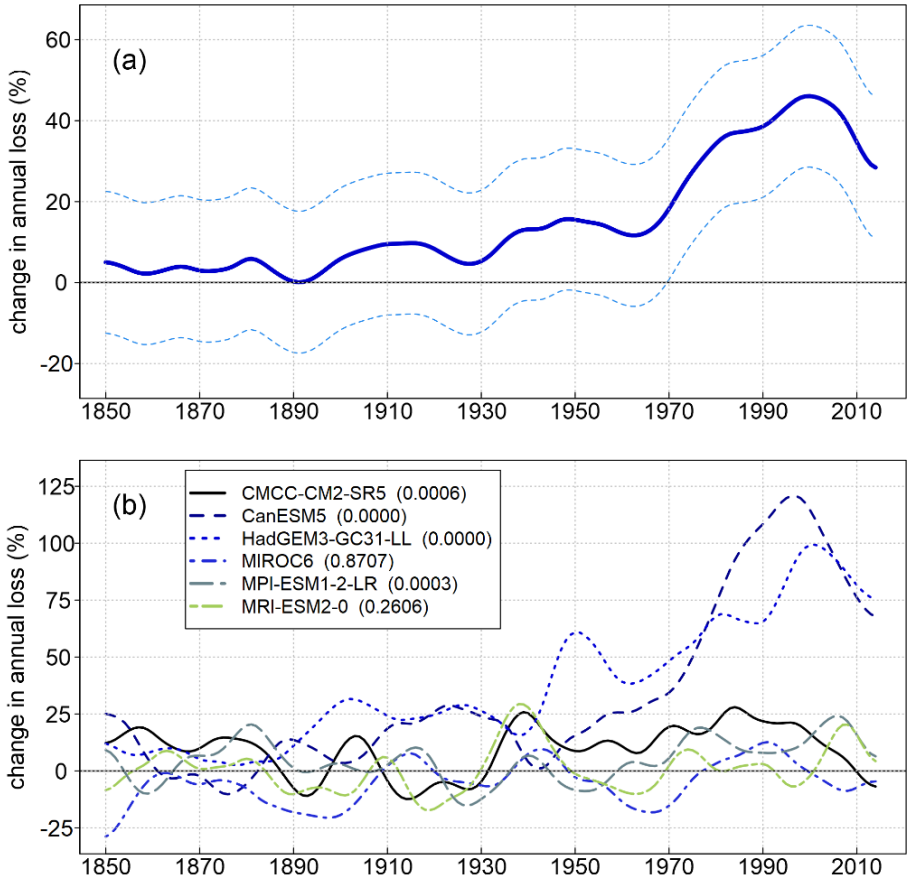

Figure 2: AA-forced change in modeled losses. (a) Timeseries of change (%) in DAMIP multimodel mean Europe-wide storm losses due to AA forcing, together with uncertainty (two standard errors of the mean, dashed lines). (b) Ensemble-mean AA forcing of European windstorm losses in each of the six climate models. The p-value of a null hypothesis that the model has zero anomaly in the 1970-2009 period is given in the legend.

https://doi.org/10.5194/egusphere-2025-6232
Preprint. Discussion started: 12 February 2026

The evolution of circulation anomalies through the 20th century are summarised in Figure 3, showing anomalies in the 500 hPa geopotential heights (ϕ_{500}) for the 30-year period 1970-99 versus the earlier, less stormy 1940-69 period, for the DAMIP-AA multimodel mean, ERA5, and ensemble means from each of the six DAMIP-AA models. The top-left panel of Figure 4 indicates how the DAMIP-AA multimodel mean contains significant meridional gradients of ϕ_{500} anomalies over the northern Atlantic area, with an amplitude of about 12 m. This anomalous gradient is about one-third of the magnitude in the ERA5 reconstruction (top-right panel of Figure 4). This relativity between model and observed is similar for storm losses, where the multimodel anomaly (Figure 2) is roughly one-quarter of that from an extended set of storm loss reconstructions in Cusack (2023). Further, the individual model means show a similar consistency: their changes in losses in Figure 3 are generally aligned with the size of the model's meridional gradients in ϕ_{500} anomalies, with CanESM5 containing the steepest gradient in ϕ_{500} anomalies, etc. In brief, storminess changes are generally consistent with circulation anomalies through the 20th century.

https://doi.org/10.5194/egusphere-2025-6232
Preprint. Discussion started: 12 February 2026

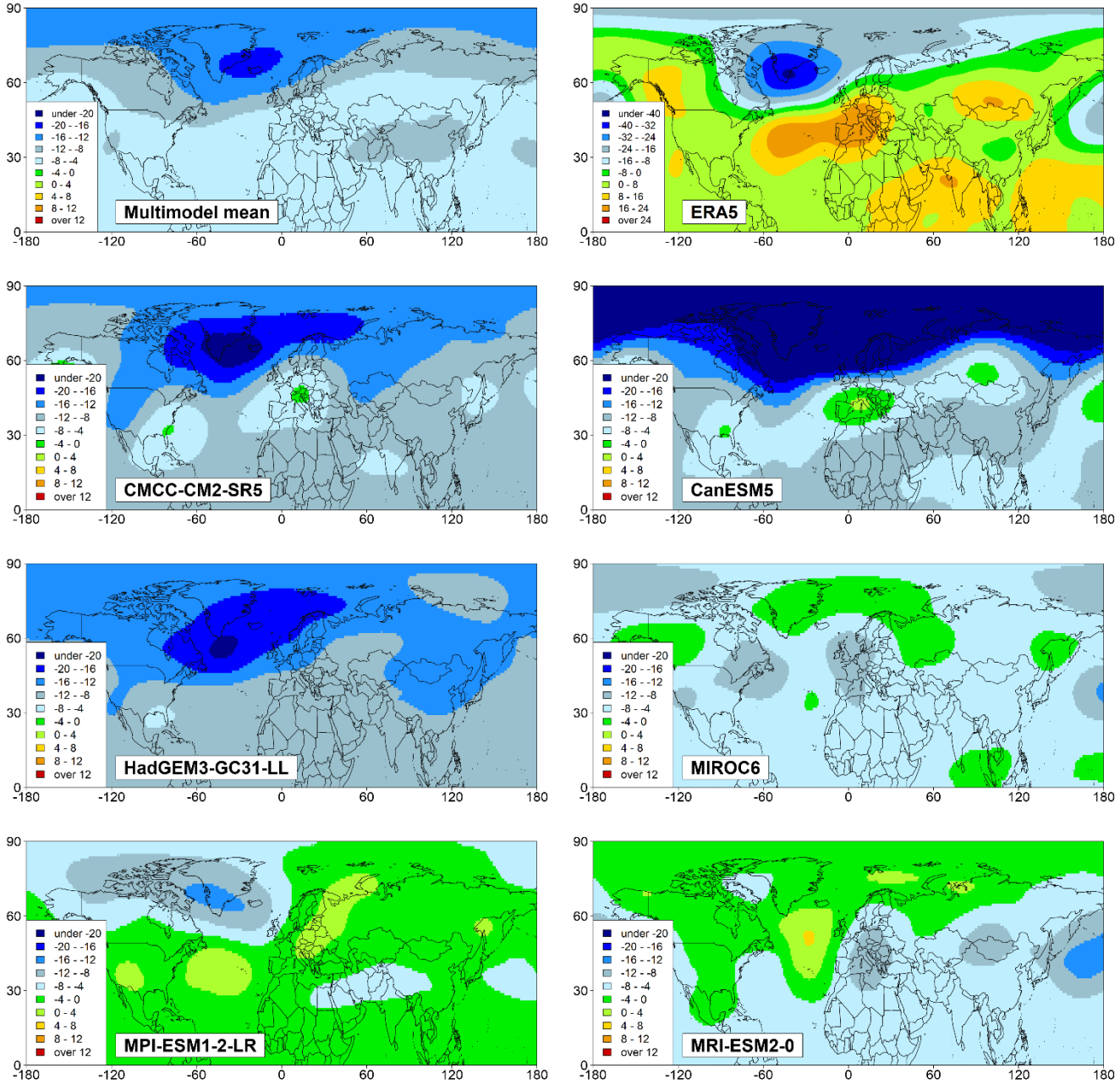

Figure 3: geopotential height anomalies at 500 hPa (m) for the 1970-1999 period relative to 1940-1969, for the DAMIP-AA multimodel-mean (top-left panel) and ERA5 (top-right panel), and the six individual DAMIP-AA model ensemble means.

170

https://doi.org/10.5194/egusphere-2025-6232
Preprint. Discussion started: 12 February 2026

4 Discussion

The spread in DAMIP-AA results suggests large uncertainty in the size of the AA forcing of European windstorm losses. For example, just 4 of 6 models produce a significant forcing of European windstorm losses, and the mean signal is largely determined by only two models. We review findings from climate research studies in this section, with the intention of bringing new information and reducing uncertainty in the AA forcing of windstorm losses.

The review begins by examining the strength of AA radiative forcing at the top-of-atmosphere in models and observed, using the global effective radiative forcing (ERF) diagnostic. Forster et al. (2021) provided a summary of the latest modelling and observational estimates of AA ERF at 2014, relative to the pre-industrial period, and includes four of the six models used in this study. Table 2 presents the data for these four models (extracted from table 7.6 of Forster et al., 2021). The IPCC authors also provide a best observational estimate of -1.3 Wm^{-2}. The mean of the four models is -1.12 Wm^{-2}, which is 13% smaller magnitude than observed and suggests the DAMIP-AA ensemble used here may underestimate true AA forcing, on average. Further, the values in Table 2 show little alignment between global AA ERF values and storm loss changes for these four models. This is illustrated by both MIROC6 and MRI-ESM2-0 having the smallest storm changes in Figure 2b, yet their ERF values are the smallest and largest values of the four models, respectively. Moreover, the spread in global AA ERF between the four models is within 12% of the mean, and much smaller than the spread in their loss impacts. In conclusion, the studied models have slightly weaker global radiative forcing from AA than best observational estimates, and the inter-model differences in strength of global ERF do not explain differences in their AA-forced storm loss anomalies.

Table 2. DAMIP-AA climate model diagnostics. Global top-of-atmosphere effective radiative forcings are from Forster et al. (2021). The difference in the AMOC trends between 1950-1990 (increases) and 1990-2020 (reductions) are from Hassan et al. (2021). The final column shows the AA-forced windstorm loss anomalies in the 1970-1999 period relative to corresponding control runs, from results presented in Sect. 3.

Model	Global AA forcing (ERF, Wm^{-2})	Change in AMOC trends (%)	1970-1999 loss anomaly (%)
CMCC-CM2-SR5	---	---	23.0
CanESM5	-1.11	8	87.2
HadGEM3-GC31-LL	-1.17	13	69.3
MIROC6	-0.99	21	4.3
MPI-ESM1-2-LR	---	10	11.3
MRI-ESM2-0	-1.22	58	5.9

https://doi.org/10.5194/egusphere-2025-6232
Preprint. Discussion started: 12 February 2026

The next step is to explore how AA radiative forcings affect the climate system. Needham and Randall (2023) framed this problem in terms of zonal-mean poleward energy transport (PET), and analysed how the radiative forcing perturbed the energy flows between zones at a planetary scale. While this study concerns impacts specific to the European sector, the zonal-mean scale of their analysis is consistent with the observed zonal scale of storm track anomalies in the late 20th century (e.g. Chang and Fu, 2002; Woollings et al., 2014), hence zonal-scale findings are relevant to recent multidecadal variations in European windstorm.

Needham and Randall (2023) showed how ERA5 total PET values in northern mid-latitudes increased from 1959 to the 1980s, then declined to 2014, and how PET anomalies from CESM2 historical simulations were consistent with ERA5 observational estimates. They proceeded to analyse various CESM2 external forcing experiments, and found AA forcing to be the main cause of the rise then fall of PET values in northern mid-latitudes from the mid-20th century to the present-day. Needham et al. (2024) broke down the total PET into more detailed component parts, and their Figures 3c and d indicate how the northern mid-latitude heat transport anomalies in the 1960-1989 period were mainly caused by the North Atlantic Ocean heat transport (via the Atlantic Meridional Overturning Circulation, AMOC), together with a smaller contribution from atmosphere eddies. In brief, the observed increase of PET in northern mid-latitudes from the mid- to late 20th century was driven by AA forcing, and was manifested as increases in both AMOC and storm track intensity.

Menary et al. (2020) described how AMOC changes over the past several decades simulated by an ensemble of CMIP6 models were likely to be larger than observed. Hassan et al. (2021) provides quantitative information on the AMOC trends for a selection of CMIP6 models in two periods, one of which has an upward trend (1950-1990) and the other with a declining trend (1990-2020), and they present data for five of the six DAMIP-AA models studied here. We use the difference in their trends (%) from the earlier to later period (i.e. [1950-1990 trend] minus [1990-2020 trend]) as a measure of a model's AMOC responsiveness to change in AA forcing, and results are listed in Table 2. These tabulated values contain a pattern, whereby models with greater AMOC changes have smaller European windstorm loss changes in the late 20th century. For example, the two models with the smallest change in storminess (MRI-ESM2-0 and MIROC6) have the largest change in AMOC trend (58% and 21% respectively), while the two models with the largest change in storm losses (CanESM5 and HadGEM3-GC31-LL) have smaller changes in AMOC strength (8% and 13% respectively). Moreover, Hassan et al. (2021) identified CanESM5 as one of the two models in their ensemble of 24 CMIP6 models which were consistent with observed AMOC trends over the past 90 years, and this model simulates the largest change in storminess of the six DAMIP-AA models studied here. This suggests DAMIP-AA simulations with less responsive AMOC to AA forcing are more consistent with estimates of past AMOC changes, and Table 2 indicates this model subset produces larger storm loss changes on average.

In conclusion, the review of climate research studies suggest CMIP6 models may underestimate mid-latitude storm increases in the late 20th century, because (a) the magnitude of modelled AA forcing is smaller than best estimates of observed, and (b)

https://doi.org/10.5194/egusphere-2025-6232
Preprint. Discussion started: 12 February 2026

models tend to overestimate AMOC responses to recent AA forcing, implying an underestimate of the increase in the storm track severity in the late 20th century. However, significant sources of uncertainty remain. First, Forster et al. (2021) indicate it is very likely that global ERF due to AA forcing in 2014 lies in a range from -0.6 to -2.0 Wm^{-2}, therefore, it is possible that the models studied here have too strong AA forcing (mean of -1.12 Wm^{-2} from Table 2). Second, the total PET anomaly in response to AA forcing has been validated for the CESM2 model, however, actual PET anomalies for the six models studied here are needed to confirm the assumption that this aspect of CESM2 is representative of modern climate models. Third, past AMOC values and trends are ambiguous: direct AMOC measurements began in 2004 with the RAPID array (Rayner et al., 2011) and its value in earlier periods have large uncertainty, and it is possible that AMOC was more responsive to AA forcing than current best estimates. Finally, while the PET analysis of zonal-mean changes is consistent with the zonal scale of storm track anomalies in the late 20th century, it is likely that simulations of local Atlantic storm track processes create extra uncertainty in model storm responses displayed in Figure 2. Future research into AA forcing of storminess, including the points mentioned above, could yield a more robust estimate of the contribution of AA forcing to the pronounced multidecadal peak of wind losses in the late 20th century, and benefit those exposed to windstorm risk.

5 Conclusions

We measured the AA-forced contribution to recent multidecadal variations in European windstorm losses using results from multiple simulations of six climate models participating in the DAMIP-AA experiment. The multimodel ensemble mean had 45% higher European windstorm losses in the late 20th century relative to preindustrial times, though anomalies range from zero to 100% between models and indicate large uncertainty in the strength of AA-forced impacts.

Past climate studies provide additional information to understand the DAMIP-AA estimates of storm responses to AA forcing. First, the global ERF due to AA forcing was found to be 10 to 15% lower in models than a best estimate of observed, which would lead to a low bias in DAMIP-AA storm responses. Second, modelled AMOC responses to AA forcing are larger than best estimates of historical AMOC behaviour, which implies an underestimate of the size of storm track anomalies in the late 20th century, also suggesting the DAMIP-AA storm responses may be biased low.

Significant uncertainties remain. For example, past values of both global ERF and AMOC are unclear and provide weak constraints on the modelled storm responses to AA forcing, while zonal-mean diagnostics cannot resolve local processes in the Atlantic sector which may modulate European storminess. Future research into these uncertainties could lead to a better understanding of multidecadal storminess in Europe and its future trajectory, and better management of this risk.

Acknowledgments

The author thanks Tyler Cox and Matt Raywood for their helpful comments during development of this manuscript.

https://doi.org/10.5194/egusphere-2025-6232
Preprint. Discussion started: 12 February 2026

Code and Data Availability

CMIP6-DAMIP climate model results were downloaded from the Earth System Grid Federation (ESGF): https://aims2.llnl.gov/search/cmip6/ (accessed July-August 2024). Model data references are as follows: CMCC-CM2-SR5 (Lovato & Peano, 2020 and 2024); CanESM5 (Swart et al., 2019a, b); HadGEM3-GC31-LL (Ridley et al., 2018; Jones, 2019); MIROC6 (Tatebe & Watanabe, 2018; Shiogama, 2019); MPI-ESM1-2-LR (Wieners et al., 2019; Müller et al., 2019); MRI-ESM2-0 (Yukimoto et al., 2019a, b).

The dataset of Europe windstorm loss reconstructions is described in Cusack (2023), with licensing restrictions, and are not accessible to the public or research community. Contact Stormwise Ltd at information@stormwise.co.uk to obtain access.

All analyses were performed using R Statistical Software (v4.2.2; R Core Team, 2022), and the low-pass filtering used the dplR package (v1.7.4; Bunn et al., 2022).

Competing interests

The author declares no competing interest.

References

Aizawa, T., Oshima, N., and Yukimoto, S.: Contributions of anthropogenic aerosol forcing and multidecadal internal variability to mid-20th century Arctic cooling—CMIP6/DAMIP multimodel analysis, Geophys. Res. Lett., 49, e2021GL097093, https://doi.org/10.1029/2021GL097093, 2022.

Ammann, C. M., and Naveau, P.: Statistical analysis of tropical explosive volcanism occurrences over the last 6 centuries, Geophys. Res. Lett., 30, 1210, https://doi.org/10.1029/2002gl016388, 2003.

Baldwin, M. P., Gray, L. J., Dunkerton, T. J., Hamilton, K., Haynes, P. H., Randel, W. J., Holton, J. R., Alexander, M. J., Hirota, I., Horinouchi, T., Jones, D. B. A., Kinnersley, J. S., Marquardt, C., Sato, K., and Takahashi, M.: The quasi-biennial oscillation, Rev. Geophys., 39, 179–229, https://doi.org/10.1029/1999RG000073, 2001.

Bauer, S. E., Tsigaridis, K., Faluvegi, G., Nazarenko, L., Miller, R. L., Kelley, M., & Schmidt, G.: The turning point of the aerosol era, J. Adv. Model. Earth Syst., 14, e2022MS003070. https://doi.org/10.1029/2022MS003070, 2022.

Birkel, S. D., Mayewski, P. A., Maasch, K. A., Kurbatov, A. V., and Lyon, B.: Evidence for a volcanic underpinning of the Atlantic multidecadal oscillation, npj Clim. Atmos. Sci., 1, 24, https://doi.org/10.1038/s41612-018-0036-6, 2018.

Böning, C. W., Scheinert, M., Dengg, J., Biastoch, A., and Funk, A.: Decadal variability of subpolar gyre transport and its reverberation in the North Atlantic overturning, Geophys. Res. Lett., 33, L21S01, https://doi.org/10.1029%2F2006GL026906, 2006.

Booth, B. B. B., Dunstone, N. J., Halloran, P. R., Andrews, T., and Bellouin, N.: Aerosols implicated as a prime driver of twentieth-century North Atlantic climate variability, Nature, 484(7393), 228–232, https://doi.org/10.1038/nature10946, 2012.

https://doi.org/10.5194/egusphere-2025-6232
Preprint. Discussion started: 12 February 2026

Brayshaw, D. J., Woollings, T., and Vellinga, M.: Tropical and extratropical responses of the North Atlantic atmospheric circulation to a sustained weakening of the MOC, J. Climate, 22, 3146–3155, https://doi.org/10.1175/2008JCLI2594.1, 2009.

Brázdil, R., Dobrovolny, P., Stekl, J., Kotyza, O., Valasek, H., & Jaroslav, J.: History of weather and climate in the Czech lands VI: Strong winds. Masaryk University, Brno, Czech Republic, 378 pp., ISBN 80-210-3547-1, 2004.

Brönnimann, S.: Impact of El Niño–Southern Oscillation on European climate, Rev. Geophys., 45, RG3003, https://doi.org/10.1029/2006rg000199, 2007.

Brönnimann, S., Franke, J., Valler, V., Hand, R., Samakinwa, E., Lundstad, E., Burgdorf, A.-M., Lipfert, L., Pfister, L., Imfeld, N., and Rohrer, M.: Past hydroclimate extremes in Europe driven by Atlantic jet stream and recurrent weather patterns, Nat. Geosci., 18, 246–253, https://doi.org/10.1038/s41561-025-01654-y, 2025.

Buckley, M. W., and Marshall, J.: Observations, inferences, and mechanisms of the Atlantic Meridional Overturning Circulation: A review, Rev. Geophys., 54, 5–63, https://doi.org/10.1002/2015RG000493, 2025

Bunn, A., Korpela, M., Biondi, F., Campelo, F., Mérian, P., Qeadan, F., and Zang, C.: dplR: Dendrochronology Program Library in R. R package version 1.7.4, https://CRAN.R-project.org/package=dplR, 2022.

Center for International Earth Science Information Network - CIESIN - Columbia University: Gridded Population of the World, Version 4.11: Population Count, Revision 11, Palisades, NY: NASA Socioeconomic Data and Applications Center (SEDAC), https://doi.org/10.7927/H4JW8BX5, 2018.

Chang, E. K. M., and Fu, Y.: Interdecadal variations in Northern Hemisphere winter storm track intensity, J. Climate, 15, 642–658, https://doi.org/10.1175/1520-0442(2002)015<0642:IVINHW>2.0.CO;2, 2002.

Cusack, S.: A long record of European windstorm losses and its comparison to standard climate indices, Nat. Hazards Earth Syst. Sci., 23, 2841–2856, https://doi.org/10.5194/nhess-23-2841-2023, 2023.

Dai, Z., Wang, B., Zhu, L., Liu, J., Sun, W., Li, L., Lü, G., Ning, L., Yan, M., and Chen, K.: Atlantic multidecadal variability response to external forcing during the past two millenniums, J. Climate, 35(24), 1–27, https://doi.org/10.1175/jcli-d-21-0986.1, 2022.

Dawson, A. G., Hickey, K., McKenna, J. and Foster, D. L.: A 200-year record of gale frequency, Edinburgh, Scotland: possible link with high-magnitude volcanic eruptions, The Holocene, 7(3), 337-341, https://doi.org/10.1177/095968369700700310, 1997.

Diao, C., Xu, Y., and Xie, S.-P.: Anthropogenic aerosol effects on tropospheric circulation and sea surface temperature (1980–2020): separating the role of zonally asymmetric forcings, Atmos. Chem. Phys., 21, 18499–18518, https://doi.org/10.5194/acp-21-18499-2021, 2021.

Eyring, V., Bony, S., Meehl, G. A., Senior, C. A., Stevens, B., Stouffer, R. J., and Taylor, K. E.: Overview of the Coupled Model Intercomparison Project Phase 6 (CMIP6) experimental design and organization, Geosci. Model Dev., 9, 1937–1958, https://doi.org/10.5194/gmd-9-1937-2016, 2016.

https://doi.org/10.5194/egusphere-2025-6232
Preprint. Discussion started: 12 February 2026

Fang, S.-W., Khodri, M., Timmreck, C., Zanchettin, D., and Jungclaus, J.: Disentangling internal and external contributions to Atlantic multidecadal variability over the past millennium, Geophys. Res. Lett., 48, e2021GL095990, https://doi.org/10.1029/2021GL095990, 2021.

Fischer E. M., Luterbacher J., Zorita E., Tett S. F. B., Casty C., and Wanner H.: European climate response to tropical volcanic eruptions over the last half millennium, Geophys. Res. Lett., 34, L05707, https://doi.org/10.1029/2006GL027992, 2007.

Forster, P., Storelvmo, T., Armour, K., Collins, W., Dufresne, J.-L., Frame, D., Lunt, D. J., Mauritsen, T., Palmer, M. D., Watanabe, M., Wild, M., and Zhang, H.: The Earth's Energy Budget, Climate Feedbacks, and Climate Sensitivity. In Climate Change 2021: The Physical Science Basis. Contribution of Working Group I to the Sixth Assessment Report of the Intergovernmental Panel on Climate Change [Masson-Delmotte, V., et al. (eds.)], Cambridge University Press, Cambridge, United Kingdom and New York, NY, USA, pp. 923–1054, https://doi.org/10.1017/9781009157896.009, 2021.

Gastineau, G., and Frankignoul, C.: Cold-season atmospheric response to the natural variability of the Atlantic meridional overturning circulation, Clim. Dynam., 39, 37–57, https://doi.org/10.1007/s00382-011-1109-y, 2012.

Gillett, N. P., Shiogama, H., Funke, B., Hegerl, G., Knutti, R., Matthes, K., Santer, B. D., Stone, D., and Tebaldi, C.: The Detection and Attribution Model Intercomparison Project (DAMIP v1.0) contribution to CMIP6, Geosci. Model Dev., 9, 3685–3697, https://doi.org/10.5194/gmd-9-3685-2016, 2016.

Gray, L. J., Woollings, T. J., Andrews, M., and Knight, J.: Eleven-year solar cycle signal in the NAO and Atlantic/European blocking, Q. J. Roy. Meteor. Soc., 142, 1890–1903, https://doi.org/10.1002/qj.2782, 2016.

Groisman, P. Y.: Possible regional climate consequences of the Pinatubo eruption: An empirical approach, Geophys. Res. Lett., 19(15), 1603–1606, https://doi.org/10.1029/92gl01474, 1992.

Gulev, S.K., Thorne, P. W., Ahn, J., Dentener, F. J., Domingues, C. M., Gerland, S., Gong, D., Kaufman, D. S., Nnamchi, H. C., Quaas, J., Rivera, J. A., Sathyendranath, S., Smith, S. L., Trewin, B., von Schuckmann, K., and Vose, R. S.: Changing State of the Climate System. In Climate Change 2021: The Physical Science Basis. Contribution of Working Group I to the Sixth Assessment Report of the Intergovernmental Panel on Climate Change [Masson-Delmotte, V., et al. (eds.)]. Cambridge University Press, Cambridge, United Kingdom and New York, NY, USA, pp. 287–422, https://doi.org/10.1017/9781009157896.004, 2021.

Hassan, T., Allen, R. J., Liu, W., and Randles, C. A.: Anthropogenic aerosol forcing of the Atlantic meridional overturning circulation and the associated mechanisms in CMIP6 models, Atmos. Chem. Phys., 21, 5821–5846. https://doi.org/10.5194/acp-21-5821-2021, 2021.

Hoesly, R. M., Smith, S. J., Feng, L., Klimont, Z., Janssens-Maenhout, G., Pitkanen, T., Seibert, J. J., Vu, L., Andres, R. J., Bolt, R. M., Bond, T. C., Dawidowski, L., Kholod, N., Kurokawa, J.-I., Li, M., Liu, L., Lu, Z., Moura, M. C. P., O'Rourke, P. R., and Zhang, Q.: Historical (1750–2014) anthropogenic emissions of reactive gases and aerosols from the Community Emissions Data System (CEDS), Geosci. Model Dev., 11, 369–408, https://doi.org/10.5194/gmd-11-369-2018, 2018.

Hu, H.-M., Trouet, V., Spötl, C., Tsai, H.-C., Chien, W.-Y., Sung, W.-H., Michel, V., Yu, J.-Y., Valensi, P., Jiang, X., Duan, F., Wang, Y., Mii, H.-S., Chou, Y.-M., Lone, M. A., Wu, C.-C., Starnini, E., Zunino, M., Watanabe, T. K., Watanabe, T., Hsu,

https://doi.org/10.5194/egusphere-2025-6232
Preprint. Discussion started: 12 February 2026

H.-H., Moore, G. W. K., Zanchetta, G., Pérez-Mejías, C., Lee, S.-Y., and Shen, C.-C.: Tracking westerly wind directions over Europe since the middle Holocene, Nature Communications, 13, 7866. https://doi.org/10.1038/s41467-022-34952-9, 2022.

Ineson, S., Scaife, A. A., Knight, J. R., Manners, J. C., Dunstone, N. J., Gray, L. J., and Haigh, J. D.: Solar forcing of winter climate variability in the Northern Hemisphere, Nat. Geosci. 4: 753–757, https://doi.org/10.1038/ngeo1282, 2011.

Jones, G.: MOHC HadGEM3-GC31-LL model output prepared for CMIP6 DAMIP hist-aer [Dataset]. Earth System Grid Federation, https://doi.org/10.22033/ESGF/CMIP6.6052, 2019.

Karremann, M. K., Pinto, J. G., von Bomhard, P. J. and Klawa, M.: On the clustering of winter storm loss events over Germany. Nat. Hazards Earth Syst. Sci., 14, 2041–2052, https://doi.org/10.5194/nhess-14-2041-2014, 2014.

Klawa, M., and Ulbrich, U.: A model for the estimation of storm losses and the identification of severe winter storms in Germany, Nat. Hazards Earth Syst. Sci., 3:725-732, https://doi.org/10.5194/nhess-3-725-2003, 2003.

Kuroda, Y., Kodera, K., Yoshida, K., Yukimoto, S., and Gray, L.: Influence of the solar cycle on the North Atlantic Oscillation, J. Geophys. Res.-Atmos., 127, e2021JD035519, https://doi.org/10.1029/2021JD035519, 2022.

Labitzke, K., and Kunze, M.: Variability in the stratosphere: The Sun and the QBO, in Climate and Weather of the Sun-Earth System. Selected Papers from the Kyoto Symposium, edited by K. S. T. Tsuda, R. Fujii and M. Geller, pp. 257 – 278, Tokyo, https://www.geo.fu-berlin.de/met/ag/strat/publikationen/docs/Labitzke-Kunze_CAWSES_TERRAPUB2009.pdf, 2009.

Leckebusch, G. C., Ulbrich, U., Fröhlich, L., and Pinto, J. G.: Property loss potentials for European midlatitude storms in a changing climate, Geophys. Res. Lett., 34, L05703, https://doi.org/10.1029/2006GL027663, 2007.

Lovato, T., and Peano, D.: CMCC CMCC-CM2-SR5 model output prepared for CMIP6 CMIP piControl [Dataset], Earth System Grid Federation, https://doi.org/10.22033/ESGF/CMIP6.3874, 2020.

Lovato, T., and Peano, D.: CMCC CMCC-CM2-SR5 model output prepared for CMIP6 DAMIP hist-aer [Dataset], Earth System Grid Federation, https://doi.org/10.22033/ESGF/CMIP6.17947, 2024.

Lund, M. T., Myhre, G., Haslerud, A. S., Skeie, R. B., Griesfeller, J., Platt, S. M., Kumar, R., Myhre, C. L., and Schulz, M.: Concentrations and radiative forcing of anthropogenic aerosols from 1750 to 2014 simulated with the Oslo CTM3 and CEDS emission inventory, Geosci. Model Dev., 11, 4909–4931, https://doi.org/10.5194/gmd-11-4909-2018, 2018.

Lund, M. T., Myhre, G., and Samset, B. H.: Anthropogenic aerosol forcing under the Shared Socioeconomic Pathways, Atmos. Chem. Phys., 19, 13827–13839, https://doi.org/10.5194/acp-19-13827-2019, 2019.

Mann, M. E., Steinman, B. A., Brouillette, D. J., and Miller, S. K.: Multidecadal climate oscillations during the past millennium driven by volcanic forcing, Science, 371, 1014–1019, https://doi.org/10.1126/science.abc5810, 2021.

Mellado-Cano, J., D. Barriopedro, R. García-Herrera, R. M. Trigo and Hernández, A.: Examining the North Atlantic Oscillation, east Atlantic pattern, and jet variability since 1685, J. Climate, 32, 6285–6298, https://doi.org/10.1175/JCLI-D-19-0135.1, 2019.

Menary, M. B., Robson, J., Allan, R. P., Booth, B. B. B., Cassou, C., Gastineau, G., Gregory, J., Hodson, D., Jones, C., Mignot, J., Ringer, M., Sutton, R., Wilcox, L., and Zhang, R.: Aerosol-forced AMOC changes in CMIP6 historical simulations, Geophys. Res. Lett., 47, e2020GL088166, https://doi.org/10.1029/2020GL088166, 2020.

https://doi.org/10.5194/egusphere-2025-6232
Preprint. Discussion started: 12 February 2026

Mignot, J., Khodri, M., Frankignoul, C., and Servonnat, J.: Volcanic impact on the Atlantic Ocean over the last millennium, Climate of the Past, 7, 1439–1455, https://doi.org/10.5194/cp-7-1439-2011, 2011.

Müller, W., Ilyina, T., Li, H., Timmreck, C., Gayler, V., Wieners, K.-H. et al.: MPI-M MPI-ESM1.2-LR model output prepared for CMIP6 DAMIP hist-aer [Dataset]. Earth System Grid Federation. https://doi.org/10.22033/ESGF/CMIP6.15024, 2019.

Needham, M. R., and Randall, D. A.: Anomalous Northward Energy Transport due to Anthropogenic Aerosols During the 20th Century, J. Climate, 36, 1–37, https://doi.org/10.1175/JCLI-D-22-0798.1, 2023.

Needham, M. R., TCox, T., and Randall, D. A.: Aerosol-Induced Changes in Atmospheric and Oceanic Heat Transports in the CESM2 Large Ensemble, J. Climate, 37, 6395–6412, https://doi.org/10.1175/JCLI-D-23-0455.1, 2014.

Omrani, N. E., Keenlyside, N. S., Bader, J., and Manzini, E.: Stratosphere key for wintertime atmospheric response to warm Atlantic decadal conditions, Clim. Dynam., 42(3-4), 649–663, https://doi.org/10.1007/s00382-013-1860-3, 2014.

Orme, L. C., Ludlow, F., Langton, N., Sjöström, J. K., Kylander, M., Murphy, C., Pyne-O'Donnell, S., Turner, J., Li, N., Davies, S. J., Mitchell, F., and Matthews, J. A.: Storminess in North West Europe and volcanic activity during the Holocene, EGUsphere [preprint], https://doi.org/10.5194/egusphere-2025-3737, 2025.

Ortega, P., Lehner, F., Swingedouw, D., Masson-Delmotte, V., Raible, C. C., Casado, M. and Yiou, P.: A model-tested North Atlantic Oscillation reconstruction for the past millennium, Nature, 523, 71–74, https://doi.org/10.1038/nature14518, 2015.

Otterå O. H., Bentsen M., Drange H., and Suo L.: External forcing as a metronome for Atlantic multidecadal variability, Nat. Geosci., 3(10), 688–694, https://doi.org/10.1038/ngeo955, 2010.

Peings, Y., and Magnusdottir, G.: Forcing of the wintertime atmospheric circulation by the multidecadal fluctuations of the North Atlantic Ocean, Environ. Res. Lett., 9(3), 034018, https://dx.doi.org/10.1088/1748-9326/9/3/034018, 2014.

Pinto, J. G., Fröhlich, E. L., Leckebusch, G. C., and Ulbrich, U.: Changing European storm loss potentials under modified climate conditions according to ensemble simulations of the ECHAM5/MPI-OM1 GCM, Nat. Hazards Earth Syst. Sci., 7, 165–175, https://doi.org/10.5194/nhess-7-165-2007, 2007.

Priestley, M. D. K., Stephenson, D. B., Scaife, A. A., Bannister, D., Allen, C. J. T., and Wilkie, D.: Forced trends and internal variability in climate change projections of extreme European windstorm frequency and severity, Q. J. Roy. Meteor. Soc., 150(765), 4933–4950, https://doi.org/10.1002/qj.4849, 2024.

Qin, M., Dai, A., and Hua, W.: Aerosol-forced multidecadal variations across all ocean basins in models and observations since 1920, Sci. Adv., 6, eabb0425, https://doi.org/10.1126/sciadv.abb0425, 2020.

R Core Team,: R: A language and environment for statistical computing [software]. R Foundation for Statistical Computing, Vienna, Austria. https://www.R-project.org/, 2022.

Rayner D., Hirschi, J. J.-M., Kanzow, T., Johns, W. E., Wright, P. G., Frajka-Williams, E., Bryden, H. L., Meinen, C. S., Baringer, M. O., Marotzke, J., Beal, L. M., and Cunningham, S. A.: Monitoring the Atlantic meridional overturning circulation, Deep Sea Res. Pt. II, 58(17–18), 1744–1753, https://doi.org/10.1016/j.dsr2.2010.10.056, 2011.

Ridley, J., Menary, M., Kuhlbrodt, T., Andrews, M., and Andrews, T.: MOHC HadGEM3-GC31-LL model output prepared for CMIP6 CMIP piControl [Dataset], Earth System Grid Federation, https://doi.org/10.22033/ESGF/CMIP6.6294, 2018.

https://doi.org/10.5194/egusphere-2025-6232
Preprint. Discussion started: 12 February 2026

Robock, A. and Mao, J.: The Volcanic Signal in Surface Temperature Observations, J. Climate, 8, 1086–1103, https://doi.org/10.1175/1520-0442(1995)008<1086:TVSIST>2.0.CO;2, 1995.

Robock, A.: Volcanic eruptions and climate, Rev. Geophys., 38, 191–219, https://doi.org/10.1029/1998RG000054, 2000.

Robson J., Sutton R., Menary M. B., and Lai M. W. K.: Contrasting internally and externally generated Atlantic Multidecadal Variability and the role for AMOC in CMIP6 historical simulations, Philos. Trans. A Math. Phys. Eng. Sci., 381: 20220194, https://doi.org/10.1098/rsta.2022.0194, 2023.

Scaife, A. A., Ineson, S., Knight, J. R., Gray, L., Kodera, K., and Smith, D. M.: A mechanism for lagged North Atlantic climate response to solar variability, Geophys. Res. Lett., 40, 434–439, https://doi.org/10.1002/grl.50099, 2013.

Shindell, D. T., Schmidt, G. A., Mann, M. E. and Faluvegi, G.: Dynamic winter climate response to large tropical volcanic eruptions since 1600, J. Geophys. Res.-Atmos., 109, D05104, https://doi.org/10.1029/2003JD004151, 2004.

Shiogama, H.: MIROC MIROC6 model output prepared for CMIP6 DAMIP hist-aer [Dataset], Earth System Grid Federation, https://doi.org/10.22033/ESGF/CMIP6.5579, 2019.

Stenchikov, G., Delworth, T. L., Ramaswamy, V., Stouffer, R. J., Wittenberg, A. and Zeng, F.: Volcanic signals in oceans, J. Geophys. Res.-Atmos., 114, D16104, https://doi.org/10.1029/2008JD011673, 2009.

Swart, N. C., Cole, J. N. S., Kharin, V. V., Lazare, M., Scinocca, J. F., Gillett, N. P., et al.: CCCma CanESM5 model output prepared for CMIP6 CMIP historical [Dataset], Earth System Grid Federation, https://doi.org/10.22033/ESGF/CMIP6.3610, 2019a.

Swart, N. C., Cole, J. N. S., Kharin, V. V., Lazare, M., Scinocca, J. F., Gillett, N. P., et al.: CCCma CanESM5 model output prepared for CMIP6 DAMIP hist-aer [Dataset], Earth System Grid Federation, https://doi.org/10.22033/ESGF/CMIP6.3597, 2019b.

Tatebe, H., and Watanabe, M.: MIROC MIROC6 model output prepared for CMIP6 CMIP piControl [Dataset], Earth System Grid Federation, https://doi.org/10.22033/ESGF/CMIP6.5711, 2018.

Thiéblemont, R., Matthes, K., Omrani, N.-E., Kodera, K., and Hansen, F.: Solar forcing synchronizes decadal North Atlantic climate variability, Nat. Comm., 6, 8268, https://doi.org/10.1038/ncomms9268, 2015.

Wang, J., Yang, B., Ljungqvist, F. C., Luterbacher, J., Osborn, T. J., Briffa, K. R., and Zorita E.: Internal and external forcing of multidecadal Atlantic climate variability over the past 1,200 years, Nat. Geosci., 10, 512–517, https://doi.org/10.1038/ngeo2962, 2017.

WASA Group: Changing waves and storms in the northeast Atlantic? B. Am. Meteorol. Soc., 79, 741–760, https://doi.org/10.1175/1520-0477(1998)079<0741:CWASIT>2.0.CO;2, 1998.

Wieners, K.-H., Giorgetta, M., Jungclaus, J., Reick, C., Esch, M., Bittner, M., et al.: MPI-M MPI-ESM1.2-LR model output prepared for CMIP6 CMIP piControl [Dataset], Earth System Grid Federation, https://doi.org/10.22033/ESGF/CMIP6.6675, 2019.

Woollings, T., Czuchnicki, C., and Franzke, C.: Twentieth century North Atlantic jet variability, Q. J. Roy. Meteor. Soc., 140, 783–791, https://doi.org/10.1002/qj.2197, 2014.

https://doi.org/10.5194/egusphere-2025-6232
Preprint. Discussion started: 12 February 2026

Woollings, T., Franzke, C., Hodson, D. L. R., Dong, B., Barnes, E. A., Raible, C. C., and Pinto, J. G.: Contrasting interannual and multidecadal NAO variability, Clim. Dynam., 45, 539–556, https://doi.org/10.1007/s00382-014-2237-y, 2015.

Yan, X., Zhang, R., and Knutson, T. R.: Underestimated AMOC variability and implications for AMV and predictability in CMIP models, Geophys. Res. Lett., 45, 4319–4328, https://doi.org/10.1029/2018GL077378, 2018.

Yukimoto, S., Koshiro, T., Kawai, H., Oshima, N., Yoshida, K., Urakawa, S., et al.: MRI MRI-ESM2.0 model output prepared for CMIP6 CMIP piControl [Dataset], Earth System Grid Federation, https://doi.org/10.22033/ESGF/CMIP6.6900, 2019a.

Yukimoto, S., Koshiro, T., Kawai, H., Oshima, N., Yoshida, K., Urakawa, S., et al.: MRI MRI-ESM2.0 model output prepared for CMIP6 DAMIP hist-aer [Dataset], Earth System Grid Federation, https://doi.org/10.22033/ESGF/CMIP6.6821, 2019b.

Zanchettin D., Timmreck, C., Bothe, O., Lorenz, S. J., Hegerl, G., Graf, H. F., Luterbacher, J., and Jungclaus, J. H.: Delayed winter warming: A robust decadal response to strong tropical volcanic eruptions? Geophys. Res. Lett., 40, 204–209, https://doi.org/10.1029/2012GL054403, 2013.

Zhang, R., Sutton R., Danabasoglu G., Kwon Y. O., Marsh R., Yeager S. G., Amrhein, D. E., and Little, C. M.: A review of the role of the Atlantic meridional overturning circulation in Atlantic multidecadal variability and associated climate impacts, Rev. Geophys., 57, 316–375, https://doi.org/10.1029/2019RG000644, 2019.